

объединенный  
институт  
ядерных  
исследований  
дубна

У432/2-81

31/8-81

E13-81-269

G.Zschornack, G.Müller, G.Musiol

**GEOMETRICAL ABERRATIONS  
IN CURVED BRAGG  
CRYSTAL SPECTROMETERS**

Submitted to "Nuclear Instruments and Methods"

**1981**

## 1. INTRODUCTION

In recent years, the technical and methodical progress on several fields has contributed to an increase in the accuracy of curved crystal spectrometers and has excluded a series of aberrations, typical for spectrometer operation. Essentially, most of aberrations which might occur with a curved crystal spectrometer can be negligible by a careful construction, alignment and operation of the spectrometer. However, the types of aberrations, which can occur, and their relative magnitudes should be noted. Some aberrations produce a line shift, others contribute only to broadening of the line. Line shifts could affect in systematic errors in the measurements of the wavelengths or energies. Especially, this problem takes a leading part at the absolute determination of the wavelengths or energies.

In the present time, wavelengths standards, which only exhibit errors from some few ppm, exist for calibration in the X-ray spectroscopy with crystal diffraction spectrometers. As a primary standard, the  $WK_{\alpha_1}$  line is used; its value was determined by  $\lambda WK_{\alpha_1} = 0.20901349(18) \text{ \AA}$  (see ref.<sup>1/</sup>).

In other papers a series of high precision secondary standards is also determined, so  $\lambda MoK_{\alpha_1} = 0.7093187(4) \text{ \AA}$  and  $\lambda CuK_{\alpha_1} = 1.5405981(15) \text{ \AA}$  in the papers of Deslattes et al.<sup>1,2/</sup>,  $\lambda AgK_{\alpha_1} = 0.5594219(9) \text{ \AA}$  and  $\lambda CrK_{\alpha_2} = 2.293665(4) \text{ \AA}$  by a combination of the results of Deslattes et al.<sup>1,2/</sup> and Bearden et al.<sup>3/</sup> and  $\lambda AlK_{\alpha_{1,2}} = 8.34034(7) \text{ \AA}$  by Henins<sup>4/</sup>. The probable errors in refs.<sup>1-3/</sup> lie at about ppm, only the  $AlK_{\alpha_{1,2}}$  wavelength determination gives an error of 9 ppm. To compare the results, obtained at different X-ray diffraction spectrometers, it's necessary, in addition to the knowledge of the crystal characteristics and the control of the crystal position by the use of laser interferometers<sup>5-7/</sup>, to investigate in detail the possible origin of systematic errors.

In this paper we investigate for the Bragg-case (Johann<sup>9/</sup> and Johansson<sup>10/</sup> version) centroid shifts and shape alterations of the diffraction line due to the finite size of source and crystal, i.e., the effect of geometrical aberrations.

This problem was approached for transmission spectrometers (Laue-case) by Schwitz et al.<sup>11/</sup> and was also taken into con-

sideration by Schult<sup>/12/</sup> and Reidy<sup>/13/</sup>. In the present paper we study the effect of geometrical aberrations under the maintenance of the improved statement of Schwitz et al.<sup>/11/</sup>. The investigation of the Bragg-case gives results for a series of configurations, differing quantitatively and qualitatively from the transmission case, so that an autonomous treatment seems to be necessary. In addition, interest for a more detailed analysis arises from the application of high precise laser interferometers for crystal position measurements and from the use of great crystals to improve the count efficiency of the spectrometer.

The present study doesn't take into consideration crystal structure effects, radiation absorption and extinction, and the effects, originated in errors of the crystal bending. For different geometrical cases the analytical expressions are deduced to describe the diffraction line shift. Further on, the problem is solved by integrating a multiple integral over the crystal and source volumes with the use of the Monte-Carlo-method. As a result, we present line shifts and shape alterations for concrete geometrical arrangements.

## 2. THE GEOMETRICAL PROBLEM AND THE EFFECTIVE ANGLE OF DIFFRACTION FOR THE JOHANN SPECTROMETER

We consider a focusing diffraction spectrometer with a concave crystal for the Bragg-case in the Johann-version<sup>/9/</sup>. The geometry of the problem is shown schematically in projection in Fig.1. The coordinates of an arbitrary emission point  $Q(x,y,z)$  of the radiation source are defined from the point  $T$  on the focal circle. In the same way the coordinates are defined for a diffraction point  $B(r,t,h)$  of the crystal from the point  $S$  on the same circle. The point  $S$  lies oppositely to the intersection  $K$  of the curvature axis in the plane which contains the focal circle. The axis of curvature as well as  $z$  and  $h$  (source and crystal heights) are perpendicular to that plane. The Bragg angle  $\theta$  appears between the rays passing through the points  $T$  and  $S$  and the crystal plane, i.e., the reference angle  $TSK$  becomes the value  $\pi/2 - \theta$ . The angles, forming with reference to the arbitrary emission and diffraction points  $Q$  and  $B$  ( $\angle QBK$ ), have the value  $\pi/2 - \theta_1$ . With respect to Fig.1 the following relations are valid

$$a = R \sin \theta, \quad (1)$$

$$b = R \cos \theta, \quad (2)$$

$$v = e \sin \delta, \quad (3)$$

$$w = e \cos \delta, \quad (4)$$

$$r = t/R, \quad (5)$$

$$\sin \delta = \sin(\theta + \tau - \arcsin \frac{x}{e}) = \frac{1}{e} [(b-y) \sin(\theta + \tau) - x \cos(\theta + \tau)], \quad (6)$$

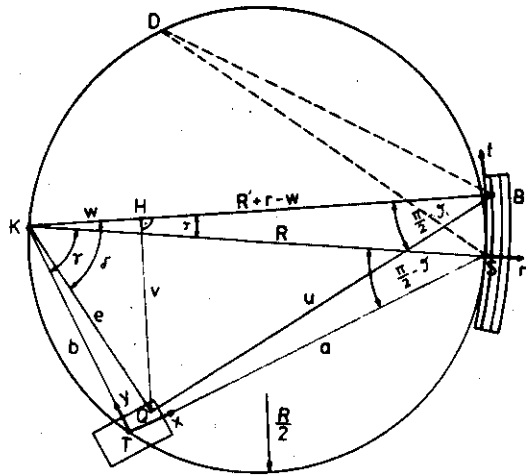
$$\cos \delta = \cos(\theta + \tau - \arcsin \frac{x}{e}) = \frac{1}{e} [(b-y) \cos(\theta + \tau) + x \sin(\theta + \tau)]. \quad (7)$$

Insertion of eqs. (6) and (7) in eqs. (3) and (4) yields:

$$v = (b-y) \sin(\theta + \tau) - x \cos(\theta + \tau), \quad (8)$$

$$w = (b-y) \cos(\theta + \tau) + x \sin(\theta + \tau). \quad (9)$$

Fig.1. Schematic geometry of a curved crystal Bragg spectrometer (Johann version). T - source reference point on the focal circle; Q - projection of an arbitrary source point (coordinates  $x, y, z$ ) on the drawing plane; H - projection of the source point Q on a plane containing the axis of curvature and the point B; K - intersection of the axis of curvature with the drawing plane; S - crystal



reference point on the focal circle; B - projection of an arbitrary diffraction point (coordinates  $r, t, h$ ) on the drawing plane; (note, that for the Johann version the point B is placed on the focal circle);  $\theta$  - spectrometer angle between the direction of a photon, emitted in T and diffracted in S and the crystal plane;  $\theta_1$  - projection of the effective diffraction angle of a photon emitted in Q and diffracted in B; R - crystal bending radius; R' is equal to R for the Johann version and equal  $R \cos \tau$  for the Johansson version.

The space between the arbitrary emission and diffraction points Q and B can be expressed as

$$u = [(R+r-w)^2 + v^2 + (h-z)^2]^{1/2}. \quad (10)$$

To take into consideration the triangle QBH,  $\sin\theta_i$  has the form:

$$\sin\theta_i = \cos\left(\frac{\pi}{2} - \theta_i\right) = \frac{R+r-w}{u} = \frac{R+r-w}{[(R+r-w)^2 + v^2 + (h-z)^2]^{1/2}}. \quad (11)$$

For a favourable mathematical treatment we define the following quantities:

$$\rho = r/R, \quad (12)$$

$$\xi = (h-z)/R, \quad (13)$$

$$\epsilon = y/R, \quad (14)$$

$$\mu = x/R, \quad (15)$$

$$v' = v/R = (\cos\theta - \epsilon) \sin(\theta + \tau) - \mu \cos(\theta + \tau), \quad (16)$$

$$w' = w/R = (\cos\theta - \epsilon) \cos(\theta + \tau) + \mu \sin(\theta + \tau). \quad (17)$$

Substituting eqs. (12) for (17) in eq. (11),  $\sin\theta_i$  is given by

$$\sin\theta_i = \frac{1 + \rho - w'}{[(1 + \rho - w')^2 + v'^2 + \xi^2]^{1/2}}. \quad (18)$$

We use formula (18) as a starting point for analytical and numerical investigations of the influence of geometrical effects on aberrations in the line position and shape alteration of diffraction lines in curved Bragg crystal spectrometers. To demonstrate the influence of single crystal dimensions, we provide an analytical study for these cases in the next chapter. The obtained expressions are very useful to estimate the effects provided by single geometrical dimensions.

### 3. POINT SOURCE AND EXTENDED CRYSTAL IN THE JOHANN SPECTROMETER

#### 3.1. Effect of the Crystal Height

We consider a source ( $x_0 = y_0 = z_0 = 0$ ) and a crystal line extending from  $-h_0/2$  to  $+h_0/2$  with  $r_0 = t_0 = 0$ . Formula (18)

becomes (with  $\xi' = \xi / \sin \theta$ ):

$$\begin{aligned} \sin \theta_i &= \frac{1 - w'}{[(1 - w')^2 + v'^2 + \xi^2]^{1/2}} = \\ &= \frac{\sin^2 \theta}{[\sin^2 \theta + \xi^2]^{1/2}} = \sin \theta \left( \frac{1}{1 + \xi'^2} \right)^{1/2}. \end{aligned} \quad (19)$$

The average value of  $\sin \theta_i$ , obtained by integration over the range  $\xi'_1 = -h_0/2a$  to  $\xi'_2 = h_0/2a$  yields:

$$\overline{\sin \theta} = \frac{\sin \theta}{\xi'_2 - \xi'_1} \int_{\xi'_1}^{\xi'_2} \left( \frac{1}{1 + \xi'^2} \right)^{1/2} d\xi'. \quad (20)$$

With  $\xi'_2 = -\xi'_1$  the average value of  $\sin \theta_i$  becomes the form

$$\overline{\sin \theta} = \frac{\sin \theta}{2\xi'_2} \ln \frac{(1 + \xi'^2)^{1/2} + \xi'_2}{(1 + \xi'^2)^{1/2} - \xi'_2}. \quad (21)$$

A series expansion of the logarithmic term in formula (21) yields:

$$\begin{aligned} \overline{\sin \theta} &= \frac{\sin \theta}{2\xi'_2} 2 \ln [(1 - \xi'^2)^{1/2} + \xi'_2] = \frac{\sin \theta}{\xi'_2} \operatorname{arcsinh} \xi'_2 = \\ &= \sin \theta \left( 1 - \frac{h_0^2}{24a^2} + \frac{3}{640} \frac{h_0^4}{a^4} - \dots \right). \end{aligned} \quad (22)$$

As it follows from formula (22), the average angle  $\bar{\theta}$  is smaller than the measured angle  $\theta$ , so that a larger one than the true wavelength is determined. The wavelength shift is

$$\frac{\Delta \lambda}{\lambda} = \frac{\Delta(\sin \theta)}{\sin \theta} = \left[ \frac{1}{24} \frac{h_0^2}{a^2} - \frac{3}{640} \frac{h_0^4}{a^4} + \dots \right] \approx \frac{1}{24} \frac{h_0^2}{R^2 \sin^2 \theta}, \quad (23)$$

where

$$\Delta(\sin \theta) = \sin \theta - \overline{\sin \theta}. \quad (24)$$

We can note an angle dependent wavelength shift, where the shift increases with  $(\sin \theta)^{-2}$ .

### 3.2. Effect of Crystal Width

We consider the case  $x_0 = y_0 = z_0 = r_0 = h_0 = 0$ . Then, formula (18) has the form

$$\begin{aligned} \sin \theta_i &= \frac{1 - \cos \theta \cos(\theta + r)}{[(1 - \cos \theta \cos(\theta + r))^2 + \cos^2 \theta \sin^2(\theta + r)]^{1/2}} = \\ &= \frac{1 - \cos \theta \cos(\theta + r)}{[1 + \cos^2 \theta - 2 \cos \theta \cos(\theta + r)]^{1/2}}. \end{aligned} \quad (25)$$

To obtain an explicit  $\sin \theta$  -dependence in formula (25), we transform eq. (25) in the form

$$\sin \theta_i = \sin \theta \frac{1 + \cot^2 \theta (1 - \cos r) + \cot \theta \sin r}{[1 + 2 \cot^2 \theta (1 - \cos r) + 2 \cot \theta \sin r]^{1/2}}. \quad (26)$$

If the angle  $r$  is assumed to be small ( $r \ll \pi/2$ ), we can write down approximately

$$1 - \cos r \approx r^2/2, \quad (27)$$

$$\sin r \approx r.$$

The insertion of eqs. (27) in eq. (26) yields:

$$\begin{aligned} \sin \theta_i &\approx \sin \theta \frac{1 + r^2/2 \cot^2 \theta + r \cot \theta}{[1 + r^2 \cot^2 \theta + 2r \cot \theta]^{1/2}} \approx \\ &\approx \sin \theta \frac{1 + r^2/2 \cot^2 \theta + r \cot \theta}{1 + r \cot \theta} \approx \frac{\sin \theta}{2} \left( 1 + r \cot \theta + \frac{1}{1 + r \cot \theta} \right). \end{aligned} \quad (28)$$

The average value of  $\sin \theta_i$  is obtained by the integration over the range from  $-t_0/2R$  to  $+t_0/2R$

$$\begin{aligned} \overline{\sin \theta} &= \sin \theta \left( \frac{1}{2} + \frac{1}{2} \frac{\int_{-t_0/2R}^{+t_0/2R} \frac{d\tau}{1 + r \cot \theta}}{t/R} \right) = \\ &= \sin \theta \left( \frac{1}{2} + \frac{1}{2} \frac{\ln \frac{1 + t_0/2R \cot \theta}{1 - t_0/2R \cot \theta}}{\frac{t_0}{R} \cot \theta} \right). \end{aligned} \quad (29)$$

Performing a series expansion of this expression, we obtain

$$\overline{\sin \theta} \approx \sin \theta \left[ 1 + \frac{1}{24} \left( \frac{t_0}{R} \cot \theta \right)^2 + \frac{1}{160} \left( \frac{t_0}{R} \cot \theta \right)^4 + \dots \right]. \quad (30)$$

Therefore, the wavelength shift is

$$\begin{aligned} \Delta\lambda &= -\lambda \left[ \frac{1}{24} \left( \frac{t_0}{R} \cot\theta \right)^2 + \frac{1}{160} \left( \frac{t_0}{R} \cot\theta \right)^4 + \dots \right] = \\ &\approx -\lambda \frac{1}{24} \frac{t_0^2}{R^2} \cot^2 \theta. \end{aligned} \quad (31)$$

Let's note that the approximate wavelength shift in eq. (31) is valid only for large angles. For small angles the fourth power term is still important. Whereas for the Laue case we obtain an angle independent wavelength shift  $\lambda^2/8$ , for the Bragg case we get an increasing negative shift, if the angle is small.

### 3.3. Effect of the Crystal Thickness

It's assumed that  $x_0 = y_0 = z_0 = h_0 = t_0 = 0$ . To simplify matters, further on we assume that the radiation on all crystal planes is diffracted with the same probability, e.g., we neglect absorption processes of the interaction of the analysed radiation with the crystal matter. Formula (18) gives

$$\begin{aligned} \sin\theta_1 &= \frac{1 + \rho - \cos^2\theta}{[(1 + \rho - \cos^2\theta)^2 + \cos^2\theta \sin^2\theta]^{1/2}} = \\ &= \frac{\rho + \sin^2\theta}{[(\sin^2\theta + \rho)^2 + \cos^2\theta \sin^2\theta]^{1/2}}. \end{aligned} \quad (32)$$

The average value of  $\sin\theta_1$  becomes then

$$\overline{\sin\theta} = \frac{1}{\rho} \int_{-\rho/2}^{+\rho/2} \frac{\rho' + \sin^2\theta}{[(\sin^2\theta + \rho')^2 + \cos^2\theta \sin^2\theta]^{1/2}} d\rho'. \quad (33)$$

Performing the integration, we get

$$\begin{aligned} \overline{\sin\theta} &= \frac{1}{\rho} \left[ \left\{ (\sin^2\theta + \frac{\rho}{2})^2 + \sin^2\theta \cos^2\theta \right\}^{1/2} - \right. \\ &\quad \left. - \left\{ (\sin^2\theta - \frac{\rho}{2})^2 + \sin^2\theta \cos^2\theta \right\}^{1/2} \right] = \\ &= \sin\theta \left[ \left( 1 + \rho + \frac{\rho^2}{4 \sin^2\theta} \right)^{1/2} - \left( 1 - \rho + \frac{\rho^2}{4 \sin^2\theta} \right)^{1/2} \right]. \end{aligned} \quad (34)$$

A series expansion of the square root yields

$$\overline{\sin \theta} = \sin \theta \left( 1 - \frac{\rho^2}{8} \cot^2 \theta \right) = \sin \theta \left( 1 - \frac{r_0^2}{8R^2} \cot^2 \theta \right). \quad (35)$$

The shift is:

$$\frac{\Delta \lambda}{\lambda} = \frac{r_0^2}{8R^2} \cot^2 \theta. \quad (36)$$

Eq. (36) is deduced for the complete description of the geometrical aberrations to describe the radiation penetration in the crystal. Since the penetration depth is very small, this contribution can be negligible in practical calculations, because their magnitude is a few orders smaller than the other contributions. Further on, in our calculations we set  $r=0$ .

#### 4. POINT CRYSTAL AND EXTENDED SOURCE IN THE JOHANN SPECTROMETER

##### 4.1. Effect of the Source Height

We consider a point crystal ( $r_0 = t_0 = h_0 = 0$ ) and a source line extending from  $-z_0/2$  to  $+z_0/2$  with  $x_0 = y_0 = 0$ . Analogous to paragraph 3.1. the wavelength shift becomes then:

$$\begin{aligned} \frac{\Delta \lambda}{\lambda} &= \frac{1}{24} \frac{z_0^2}{R^2 \sin^2 \theta} - \frac{3}{640} \frac{z_0^4}{R^4 \sin^4 \theta} + \dots \approx \\ &\approx \frac{1}{24} \frac{z_0^2}{R^2 \sin^2 \theta}. \end{aligned} \quad (37)$$

##### 4.2. Effect of the Source Width

It's assumed that  $x_0 = z_0 = r_0 = t_0 = h_0 = 0$ . Formula (18) becomes then

$$\begin{aligned} \sin \theta_i &= \frac{1 - \cos \theta (\cos \theta - \epsilon)}{\{ [1 - \cos \theta (\cos \theta - \epsilon)]^2 + \sin^2 \theta (\cos \theta - \epsilon)^2 \}^{1/2}} = \\ &= \frac{\sin^2 \theta + \epsilon \cos \theta}{[\sin^2 \theta + \epsilon^2]^{1/2}}. \end{aligned} \quad (38)$$

Now, we transform eqs. (38), so that we obtain an explicit  $\sin \theta$  -dependence:

$$\sin \theta_i = \sin \theta \frac{1 + (\epsilon \cdot \cot \theta / \sin \theta)}{[1 + \epsilon^2 / \sin^2 \theta]^{1/2}}. \quad (39)$$

The averaged value of  $\sin\theta_1$  is obtained by integration over the range from  $-\epsilon_0/2$  to  $+\epsilon_0/2$

$$\overline{\sin\theta} = \frac{\sin\theta}{\epsilon} \int_{-\epsilon_0/2}^{+\epsilon_0/2} \frac{1 + \frac{\epsilon}{\sin\theta} \cot\theta}{\left[1 + \frac{\epsilon^2}{\sin^2\theta}\right]^{1/2}} d\epsilon. \quad (40)$$

After integration the wavelength shift yields:

$$\frac{\Delta\lambda}{\lambda} = \frac{1}{24} \frac{y_0^2}{R^2 \sin^2\theta} - \frac{1}{24} \frac{y_0^4}{R^4 \sin^4\theta} + \dots = \frac{1}{24} \frac{y_0^2}{R^2 \sin^2\theta}. \quad (41)$$

#### 4.3. Effect of the Source Depth

In this case  $y_0 = z_0 = r_0 = t_0 = h_0 = 0$ . The effective value of  $\sin\theta_1$  is then

$$\sin\theta_1 = \frac{1 - \cos^2\theta - x_0 \sin\theta}{\left[(1 - \cos^2\theta - x_0 \sin\theta)^2 + (\cos\theta \sin\theta - x_0 \cos\theta)^2\right]^{1/2}} = \sin\theta. \quad (42)$$

The result of formula (42) shows that only the source depth hasn't influences on the position and shape alterations of the diffracted line.

#### 5. SUMMARY OF THE ANALYTICAL EXPRESSIONS FOR THE JOHANN VERSION

In the previous chapters we have derived analytical expressions for the contributions from the single crystal and source dimensions. A survey about the obtained results is given in Table 1.

Contrary to the results, obtained by Schwitz et al.<sup>/11/</sup> for transmission spectrometers, we obtain an angle - dependent expression for the crystal width. For all other terms, with exception of the source depth, a  $(\sin\theta)^{-2}$  -dependence is characteristic. A decrease of the wavelength shifts can be attained by increasing the diameter R of the focal circle on the strength of the typical  $R^{-2}$  -dependence.

To illustrate the order of magnitude of the various wavelength shifts, some concrete results are given in Table 2 for a standard geometry, which we'll use for all the analytical and numerical examples in the present paper.

$$\begin{array}{lll} x_0 = 0.3 \text{ mm} & y_0 = 0.1 \text{ mm} & z_0 = 10 \text{ mm} \\ r_0 = 0 \text{ mm} & t_0 = 40 \text{ mm} & h_0 = 10 \text{ mm} \end{array} \quad (43)$$

Table 1

The influence of non-zero crystal and source dimensions on the wavelength shift  $\Delta\lambda/\lambda$  (analytical expression) in the Johann spectrometer

Non-zero Crystal Dimension	Characteristic Wavelength Shift $\Delta\lambda/\lambda$	Non-zero Source Dimension	Characteristic Wavelength Shift $\Delta\lambda/\lambda$
Height $h_0$	$\frac{1}{24} \frac{h_0^2}{R^2 \sin^2 \theta}$	Height $z_0$	$\frac{1}{24} \frac{z_0^2}{R^2 \sin^2 \theta}$
Width $t_0$	$-\frac{1}{24} \frac{t_0^2}{R^2} \cot^2 \theta$	Width $y_0$	$\frac{1}{24} \frac{y_0^2}{R^2 \sin^2 \theta}$
Depth $r$	$\frac{1}{8} \frac{r_0^2}{R^2} \cot \theta$	Depth $x_0$	0

Table 2

Analytical wavelength shifts (in ppm), created by non-zero crystal or source dimensions for diffraction angles in the range of 20 up to 85 degrees. The symmetric case is assumed

Dimension	20°	30°	40°	50°	60°	70°	80°	85°
$t_0 = 40 \text{ mm}$	-1198.4	-476.3	-225.5	-111.8	-52.9	-21.0	-4.9	-1.2
$h_0 = 10 \text{ mm}$	84.8	39.7	24.0	16.9	13.2	11.2	10.2	10.0
$y_0 = 0.1 \text{ mm}$	0.0085	0.0039	0.0024	0.0017	0.0013	0.0011	0.0010	0.0009

We assume by our estimations that the two points T and R in Fig.1 were in the plane perpendicular to the axis of curvature K and that the source and the crystal were placed symmetrically with respect to the points T and R (symmetric case).

## 6. THE TREATMENT OF THE JOHANSSON VERSION

The mathematical treatment of the Johansson version is analogous to the Johann version, as described in the previous chapters. The geometrical situation is similar to the picture,

shown in Fig.1. In difference to the Johann version we must replace the quantity  $R'$  by

$$R' = R \cos r \quad (44)$$

and the diffraction point B is in all cases places closely to the Rowland circle, because the crystal is bended with the radius  $R$  and additionally ground with the radius  $R/2$ . If we neglect the radiation penetration in the crystal, the point B is placed for all cases at the Rowland circle and the coordinate  $r$  is set to zero. Due to these conceptions, eq. (10) has the form

$$u = [(R \cos r + r - w)^2 + v^2 + (h - z)^2]^{1/2}, \quad (45)$$

so that  $\sin \theta_i$  becomes:

$$\sin \theta_i = \frac{\cos r + \rho - w'}{[(\cos r + \rho - w')^2 + v'^2 + \xi^2]^{1/2}}. \quad (46)$$

Starting from eq. (46), we notice that the formulae for the influence of non-zero crystal and source dimensions, as given in Table 1, are also valid for the Johansson version. Only the treatment of the crystal width requires a new detailed analysis. In this case  $x_0 = y_0 = z_0 = r_0 = h_0 = 0$ . Formula (46) has then the form

$$\sin \theta_i = \frac{\cos r - \cos \theta \cos(\theta + r)}{[(\cos r - \cos \theta \cos(\theta + r))^2 + \cos^2 \theta \sin^2(\theta + r)]^{1/2}}, \quad (47)$$

e.g., we find

$$\sin \theta_i = \sin \theta \quad (48)$$

From eq. (48) it follows that the crystal width in the Johansson case doesn't influence the position and shape alterations of the diffracted line. This result exactly reflects the preferences of the Johansson version to the Johann case.

## 7. THE NUMERICAL PROCEDURE

The present study is limited to the aberrations produced by the finite size of the source and the crystal on the reflex profile. In our calculations we consider an idealized homogeneous crystal. At each point the diffraction pattern  $f(\theta_i)$  will depend only on the effective angle  $\theta_i$  between the incident photon direction and the reflecting planes.

Thereby, we assume that the photon emission from each point of the source occurs with the same probability and radiation absorption and extinction doesn't occur. The numerical procedure is based on the same principle as applied by Schwitz (11) et al., but for the integral, describing the situation in Bragg spectrometers. The diffraction pattern  $f(\theta_i)$  we specify by the Gaussian function:

$$f(\theta_i) = \exp\left[-\frac{(\theta_i - \theta_B)^2}{2\sigma^2}\right], \quad (49)$$

where  $\theta_B$  denotes the Bragg angle corresponding to the wavelength of the incident photon.  $\sigma$  is a free parameter depending on the mosaic spread in the crystal. Further on, we assume that the radiation is strictly monochromatic and that the spectrometer setting angle  $\theta$  is close to the corresponding Bragg angle  $\theta_B$ . The observed reflex is given by

$$F(\theta) = \frac{1}{V} \int_V \exp\left[-\frac{(\theta_i(\theta, \vec{x}) - \theta_B)^2}{2\sigma^2}\right] dV \quad (50)$$

with  $\theta$  - effective diffraction angle and  $\theta_i(\theta, \vec{x}) = \theta_i(\theta, x, y, z, r, t, h) = \theta_i$ ,  $V = 6$  - dimensional source - crystal volume. To obtain the value of the integral (45) for any geometrical condition, we define as Schwitz et al.<sup>18/</sup> and Schult<sup>19/</sup> a distribution function  $D(\hat{\theta} - \theta)$ , independent of the diffraction pattern, as follows

$$D(\hat{\theta} - \theta) = \frac{1}{V} \int_V \delta[\sin \theta_i(\theta, \vec{x}) - \sin \hat{\theta}] dV, \quad (51)$$

where  $\delta$  is the Dirac  $\delta$ -function and  $\hat{\theta}$  - an arbitrary effective diffraction angle.

To understand the significance of  $D$ , we note that  $V \cdot D(\theta - \hat{\theta}) d\hat{\theta}$  represent that part of the 6-dimensional source-crystal volume for which the effective diffraction angle ranges between  $\hat{\theta}$  and  $\hat{\theta} + d\hat{\theta}$ . Then we have:

$$F(\theta) = \int_{\hat{\theta}} D(\theta - \hat{\theta}) f(\hat{\theta}) d\hat{\theta}. \quad (52)$$

To obtain practical results, we've developed the program GEOMC<sup>14/</sup>, which calculates the problem by the Monte-Carlo method. This program allows one to solve the 6-dimensional integral for the reflex  $F(\theta)$  and generate the distribution function  $D(\theta - \hat{\theta})$ .

## 8. NUMERICAL RESULTS FOR SINGLE GEOMETRICAL DIMENSIONS

In this caption we give some numerical results, calculated with the program GEOMC<sup>14/</sup> for our chosen standard geometry. For the calculations we have placed the crystal and the source symmetrically with respect to the points S and T, respectively.

Figure 2 shows the distribution function  $D(\theta-\hat{\theta})$  for the influence of the crystal width and the influence of finite source height and width in Figure 3 and 4, respectively. We note that the function  $D(\theta-\hat{\theta})$  for the crystal and source height has the same characteristics so that it is not necessary to demonstrate both distribution functions. Whereas the finite size of the crystal depth and the source width give only a symmetric broadening of the reflex, both the crystal height and width and also the source height lead to an asymmetric deformation of the diffraction pattern.

For practical application it is very useful to study the change of the peak position, full width at half maximum and the peak amplitude over a wide range of diffraction angles  $\theta_B$ . The characteristic influence of some selected single crystal and source dimensions on the mentioned quantities is shown in Figures 5,6 and 7.

In Table 3 we give some comparisons between calculated wavelength shifts after the formulae in Table 1 and the numerical results computed with the program GEOMC. A good agreement between the analytical and numerical results can be recorded.

Table 3

Relative shifts  $\Delta(\sin\theta)/\sin\theta$ , calculated with the analytic formulae from Table 1 (AS) and numerical calculations (MC) with the Monte-Carlo Method (program GEOMC) in ppm

Dimension	30°		50°		70°		80°	
	AS	MC	AS	MC	AS	MC	AS	MC
$h_0 = 10$ mm	39.7	39.3	16.9	16.7	11.2	11.1	10.2	10.2
$t_0 = 40$ mm	-476.3	-477.4	-111.8	-111.7	-21.0	-21.0	-4.9	-4.9

## 9. NUMERICAL RESULTS FOR NON-ZERO SOURCE AND CRYSTAL DIMENSIONS

Assuming the same predictions as mentioned above, we calculate the reflex profile for the Johann (Fig.8) and the Johansson case (Fig.9).

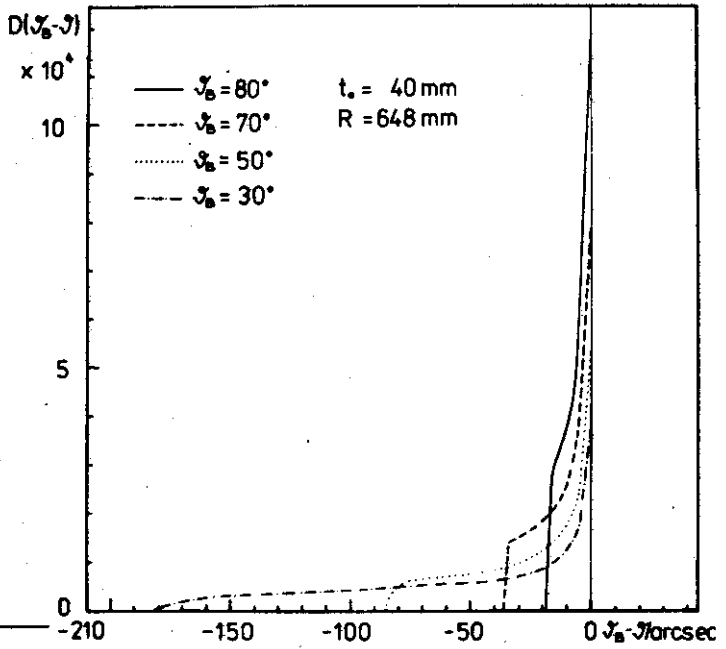


Fig.2. Distribution function  $D(\theta_B - \theta)$  in arbitrary units displaying the effect of finite crystal height.  $\sigma_0 = 5''$ .

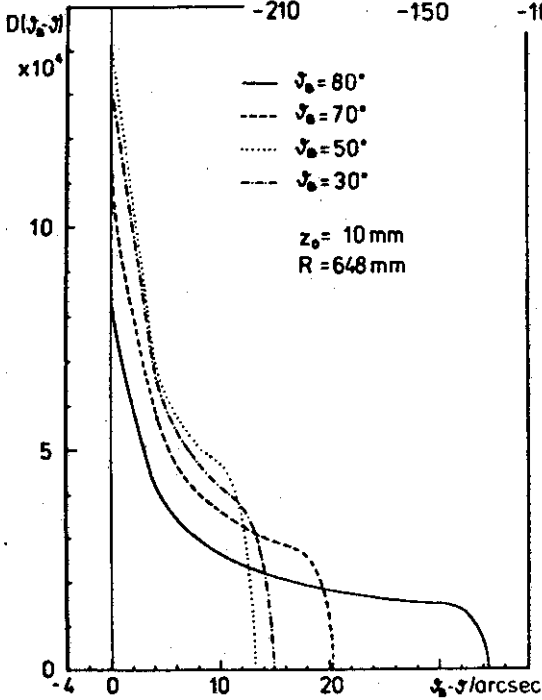
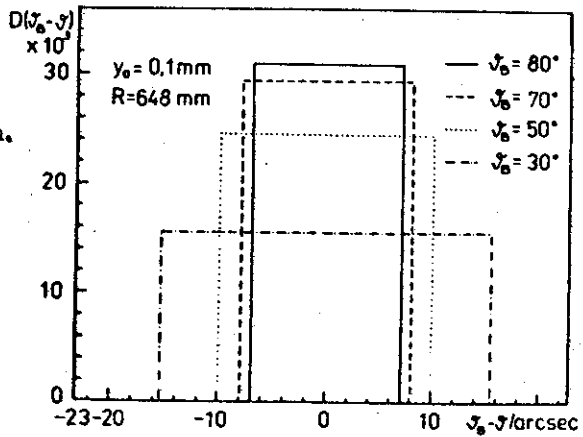
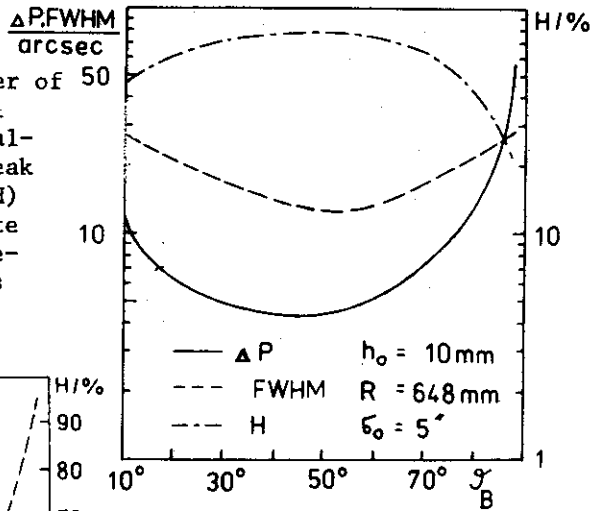
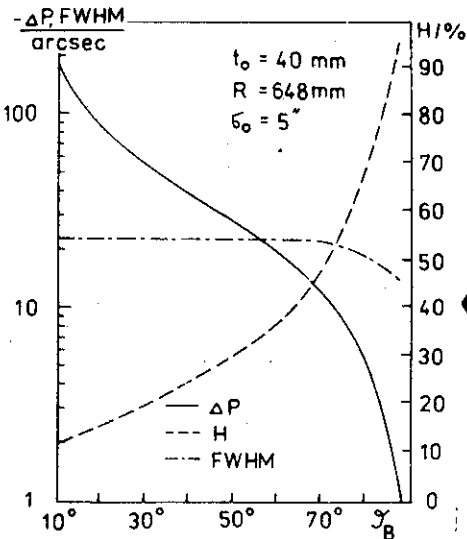


Fig.3. Distribution function  $D(\theta_B - \theta)$  in arbitrary units for the effect of finite source height.  $\sigma_0 = 5''$ .

**Fig.4.** Distribution function  $D(\theta_B - \theta)$  in arbitrary units displaying the effect of finite source width,  $\sigma_0 = 5''$ .



**Fig.5.** Calculated center of gravity shifts ( $\Delta P$ ) full width at half maximum alterations (FWHM) and peak amplitude variations (H) for the effect of finite crystal height at different diffraction angles  $\theta_B$  in Johann and Johansson spectrometers.



**Fig.6.** Calculated center of gravity shifts, full width at half maximum alterations and peak amplitude variations for the effect of finite crystal width at different diffraction angles in Johann spectrometers. For notations see explanations under fig.5.

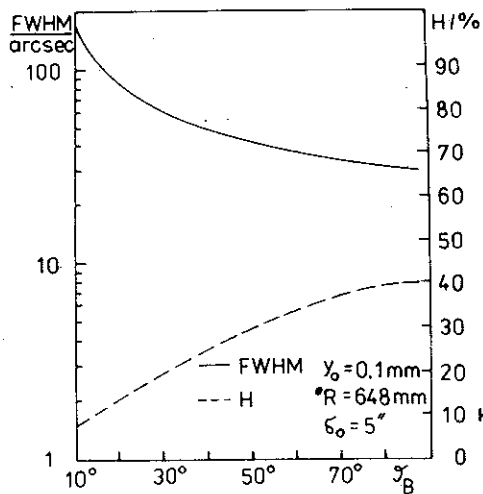


Fig. 7. Calculated full width at half maximum alterations and peak amplitude variations due to the finite size of the source width at different diffraction angles. Center of gravity shifts are not separately displayed, because their magnitude is less than 0.1 arcsec over the complete angle range. For notations see explanations under fig. 5.

Fig. 8. Reflex profile at different diffraction angles for the Johann case. The peak amplitude  $H$  is referred to Gaussian shaped diffraction pattern with the amplitude one.

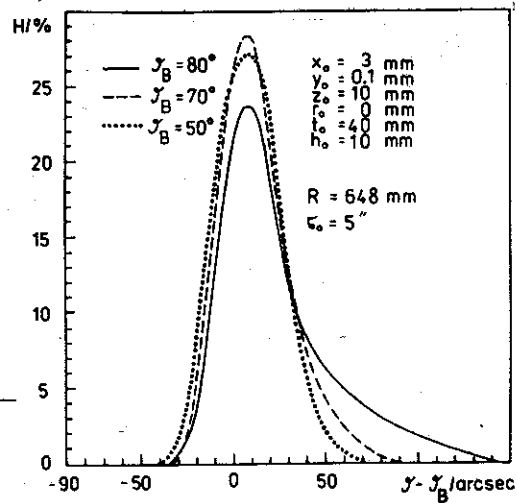
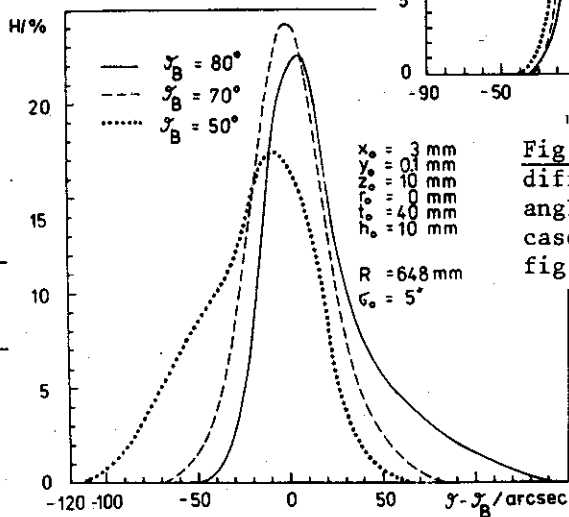


Fig. 9. Reflex profile at different diffraction angles for the Johansson case. For notations see fig. 8.

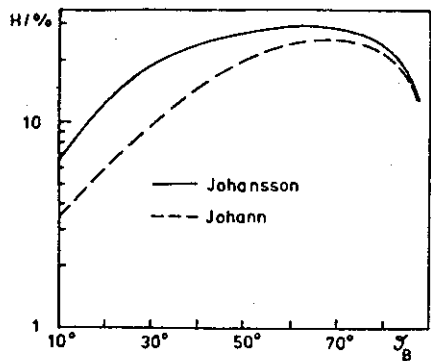


Fig. 10. Size of the reflex amplitude  $H$  after convolution with the distribution function  $D(\theta_B - \theta)$  in Johann and Johansson spectrometers. For crystal and source dimensions see eq. (43).  $R = 648$  mm,  $\sigma_0 = 5''$ .

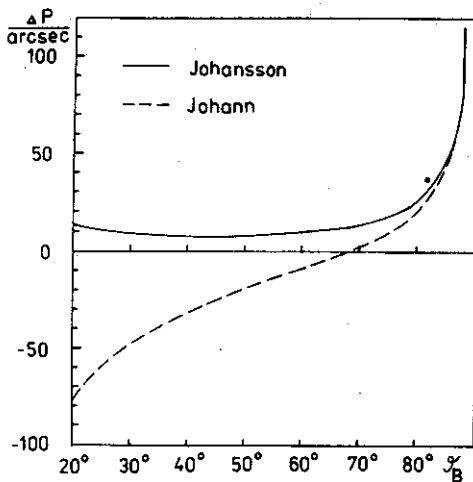


Fig. 11. Center of gravity shifts for changing diffraction angles  $\theta_B$  in Johann and Johansson spectrometers. For crystal and source dimensions see eq. (43)  $R = 648$  mm,  $\sigma_0 = 5''$ .

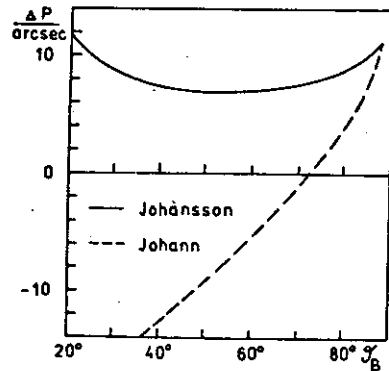


Fig. 12. Reflex maximum shifts at changing diffraction angles  $\theta_B$  in Johann and Johansson spectrometers. For crystal and source dimensions see eq. (43).  $R = 648$  mm,  $\sigma_0 = 5''$ .

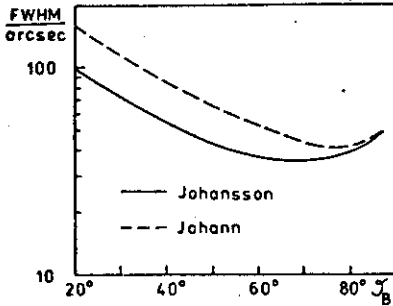


Fig.13 Full width at half maximum for various diffraction angles  $\theta_B$  in Johann and Johansson version. For crystal and source dimensions see eq. (43).  $R = 648 \text{ mm}$ ,  $\sigma_0 = 5''$ .

The size of the peak amplitude after convolution with the distribution function  $D(\theta_B - \theta)$  is presented in Fig.10. Note that the absolute maximum of the Gaussian shaped diffraction pattern becomes only less than 30 percent of the initial peak amplitude after the convolution with the distribution function.

Fig.11 demonstrates the characteristic position change of the center of gravity for changing reflection angle  $\theta_B$ . Since the peaks show in general a clear asymmetry, we demonstrate (Fig.12) the position change of the peak maxima as a function of the reflection angle  $\theta_B$ . The characteristic full width at half maximum spread is shown in Fig.13.

In Fig.8 it's seen that with the decreasing reflection angle the nearly symmetric reflex profile becomes a more asymmetrical character that can lead to complications for exact wavelength determinations in several experiments. From Figs. 10 to 13 it follows that the angle region between  $40^\circ$  and  $80^\circ$  in the Johansson case is recommended for optimal spectrometer operation. The operation of the Johann spectrometers characterizes an angle dependent position change that can lead to over- or underestimation of the analyzed wavelengths.

In all cases the shifts are mainly affected due to the crystal width and to the source and crystal heights. For all non-zero dimensions we find the following result:

$$\frac{\Delta(\sin \theta)}{\sin \theta} = \frac{\Delta \lambda}{\lambda} = \frac{1}{24} \frac{1}{R^2 \sin^2 \theta} [h_0^2 + z_0^2 + y_0^2 + 3r_0^2 \sin \theta \cos \theta - t_0^2 \cos^2 \theta]. \quad (53)$$

The shifts computed by the above-mentioned formula, can be compared with the results computed with the program GEOMC. A good agreement can be noted.

## 10. FINAL REMARKS

In this paper we have analyzed the effects caused by geometrical aberrations in Bragg diffraction spectrometers. The described theory allows one to study the influence of single geometrical dimensions on the reflex profile and position in curved crystal diffraction spectrometers. The presented method gives a uniform mathematical treatment for Bragg spectrometers in the Johann- and Johansson version. In concrete measurements it might be necessary to correct the data with the use of relation (53). The correction may be important when large crystals are used, since the geometrical parameters appear in second power. Exact knowledge about geometrical aberrations allows one to take into consideration these effects at the processing of the X-ray spectra. It may be also advantageous for estimations to find an optimum of source and crystal dimensions by the construction of concrete diffraction spectrometers.

## REFERENCES

1. Kessler E.G., Deslattes R.D., Henins A. Phys.Rev., 1979, 19, p.215.
2. Deslattes R.D., Henins A. Phys.Rev.Lett., 1973, 31, p.972.
3. Bearden J.A. et al. Phys.Rev., 1964, 134, No.4A, p.899.
4. Henins A. Proc. Int. Conf. NBS on Precision Measurement and Fundamental Constants, Maryland, USA, 1970, N.B.S. Publ. 343, August 1971, p.255.
5. Schwitz W. Nucl.Instr. and Meth., 1978, 154, p.95.
6. Marzolf J.G. Rev.Sci.Instr., 1964, 35, p.1212.
7. Deslattes R.D. Reference Wavelengths - Infrared to Gamma Rays, Avagadro's Constant, Mass and Density. In: Lectures of the Summer School of Physics Enrico Fermi, Varenna, Italy, July 12-24, 1976.
8. Borchert G.L., Scheck W., Schult O.W.B. Nucl.Instr.Meth., 1975, 124, p.107.
9. Johann H.H. Z.Phys., 1931, 69, p.185.
10. Johansson T. Z.Phys., 1933, 82, p.507.
11. Schwitz W., Kern J., Lanners R. Nucl.Instr. and Meth., 1978, 154, p.105.
12. Schult O. Z.Phys., 1960, 158, p.444.
13. Reidy J.J. In: The Electromagnetic Interaction in Nuclear Spectroscopy. North Holland, Amsterdam, 1975, p.839.
14. Zschornack G., Müller G., Musiol G. JINR, E11-81-88, Dubna, 1981.

Received by Publishing Department  
on April 21 1981.